Core expansion of bis-calix[4]arene-supported clusters

Chemical Communications

COMMUNICATION

Core expansion of *bis*-calix[4]arene-supported clusters

Marco Coletta,[a] Ross McLellan,[a] Amy Waddington,[a] Sergio Sanz,[b] Kevin J. Gagnon,[c] Simon J. Teat,[c] Euan K. Brechin*[b] and Scott J. Dalgarno*[c]

Received 00th January 20xx,
Accepted 00th January 20xx

DOI: 10.1039/x0xx00000x

www.rsc.org/

Calix[4]arenes are excellent ligand supports for the synthesis of polymetallic clusters of transition and lanthanide metal ions, as well as 3*d*-4*f* ion mixtures. Bis-calix[4]arene, a recent addition to the calixarene family, forms structurally related cages that mirror the metal ion binding preferences of calix[4]arene. Here we show that stoichiometric control causes remarkable expansion in the cores of two known *bis*-calix[4]arene-supported clusters, with concomitant changes to the magnetic properties observed.

Polymetallic clusters that exhibit interesting magnetic properties have been synthesised from a wide range of ligands, exploiting equally diverse synthetic strategies such as ambient, solvothermal and microwave temperature regimes.[1] Rational ligand design, an approach based partly on targeted metal ion binding, continues to be one of the most valuable strategies employed as one can, for example, influence cluster composition and thus the prevailing magnetic properties.[2]

We (amongst others) have recently shown that methylene-bridged calix[4]arenes (e.g. *p*-^{t}Bu-calix[4]arene and *p*-H-calix[4]arene, termed collectively as C[4]s herein) are incredibly versatile ligands for the synthesis of polymetallic clusters, with a wide variety of structural motifs arising from reactions involving transition metal (TM),[3] lanthanide metal (Ln)[4] and 3*d*-4*f* ion combinations.[5] Through our experiments we have established a vast library of polymetallic clusters in which $[C[4]TM^{III}]^-$, $[C[4]TM^{II}]^{2-}$ or $[C[4]Ln^{III}]^-$ moieties act as capping vertices in polyhedra.[6] The generic C[4] polyphenolic pocket binds particular metal ions preferentially depending on those present in the reaction mixture, with the phenolates also bridging to other metal centres within the resulting cluster core; as a result of these studies we have established a reliable set of empirical metal ion binding rules for C[4]s. With respect to the current contribution it is pertinent to mention our first result in this area, that being the synthesis and characterisation of a family of $[Mn^{III}_2Mn^{II}_2(C[4])_2]$ single molecule magnets (SMMs), all of which possess a common butterfly-like $\{Mn^{III}_2Mn^{II}_2(OH)_2\}$ core (**1**, Fig. 1A).[3b-3c] The oxidation state distribution in this general core is unusual in that it is reversed relative to the majority of those previously reported in the literature.[7] The body ions of **1** are in the 2+ oxidation state, whilst those housed in the C[4] lower-rim polyphenolic pockets at the wing-tip positions are 3+. Building on that result, we found that it was possible to systematically interchange the body Mn^{II} ions with either one or two Ln^{III} ions through variation in the metal salts, stoichiometry and reaction conditions employed (e.g. changes in solvent); this affords butterflies with $\{Mn^{III}_2Mn^{II}Ln^{III}(OH)_2\}$ and $\{Mn^{III}_2Ln^{II}_2(OH)_2\}$ cores respectively.[8] Similar reactions performed in the absence of $TM^{II/III}$ ions led to Ln^{III}_6TBC[4] octahedra,[4] while a series of $Mn^{III}_4Ln^{III}_4$TBC[4] clusters (**2**, Fig 1B) were obtained in the presence of both TM and Ln ions. The latter are best described as four $[C[4]Mn^{III}]^-$ moieties capping the edges of a square of Ln^{III} ions (Ln = Gd, Tb, Dy).[5a]

Bis-*p*-^{t}Bu-calix[4]arene (Bis-TBC[4], L1, Fig. 1C) recently emerged as a new addition to the family of calixarenes.[9] With the aforementioned coordination chemistry in mind, direct C[4] linking *via* the methylene bridge suggested to us that this ligand may be an excellent tool for controlling cluster formation.[10] For example, we anticipated that L1 would be conformationally flexible and thus be capable of behaving as a double capping species given the likely formation of bis-$[C[4]Mn^{III}]^-$ moieties. Our initial investigations with L1 confirmed this hypothesis, and clusters isolated with this ligand to date have all mirrored the coordination chemistry of isolated C[4]. Two previously reported L1-supported clusters are relevant to this contribution, the first being of formula $[Mn^{III}_4Mn^{II}_4(L1\text{-}8H)_2(\mu_3\text{-}OH)_2(\mu\text{-}OH)(\mu\text{-}Cl)(H_2O)(MeOH)(dmf)_4]$ (**3**, Fig. 1D).[11] The polymetallic core in **3** can be thought of as two distorted and fused $\{Mn^{III}_2Mn^{II}_2\}$ butterfly cores, as can be seen by comparing Figure 1A and 1D. The main structural differences observed are that, upon linking *via* the methylene bridge, the Mn^{II} ions now occupy positions between the

[a] Institute of Chemical Sciences, Heriot-Watt University, Riccarton, Edinburgh, Scotland, EH14 4AS, UK. E-mail: S.J.Dalgarno@hw.ac.uk
[b] EaStCHEM School of Chemistry, The University of Edinburgh, David Brewster Road, Edinburgh, Scotland EH9 3FJ, UK. E-mail: ebrechin@ed.ac.uk
[c] Station 11.3.1, Advanced Light Source, Lawrence Berkeley National Laboratory, 1 Cyclotron Road, Berkeley, CA94720, USA.
† We thank the EPSRC for financial support of this work under grant reference EP/I03255X/1. The Advanced Light Source is supported by the Director, Office of Science, Office of Basic Energy Sciences, of the US Department of Energy under contract no DE-AC02-05CH11231..
Electronic Supplementary Information (ESI) available: Experimental and additional figures to support discussion. See DOI: 10.1039/x0xx00000x

constituent C[4] lower-rims, and that all of the $Mn^{II/III}$ ions are linked by bridging phenolates and hydroxides; the additional pockets / binding positions for the Mn^{II} ions are generated by inversion of L1, as can be seen by comparing conformations in Figure 1C and 1E. The second notable example is the $[Mn^{III}_4Mn^{II}_2Gd^{III}_2(L1\text{-}8H)_2(Cl)_2(\mu_3\text{-}OH)_4(MeOH)_2(dmf)_8]$species (**4**) shown in Figure 1E, which represents two distorted and fused $\{Mn^{III}_2Mn^{II}Ln^{III}\}$ butterfly cores. Four Mn^{III} ions occupy the C[4] pockets as expected, and two of the four Mn^{II} ions in **3** are interchanged with Ln^{III} ions, mirroring the coordination chemistry of isolated C[4].

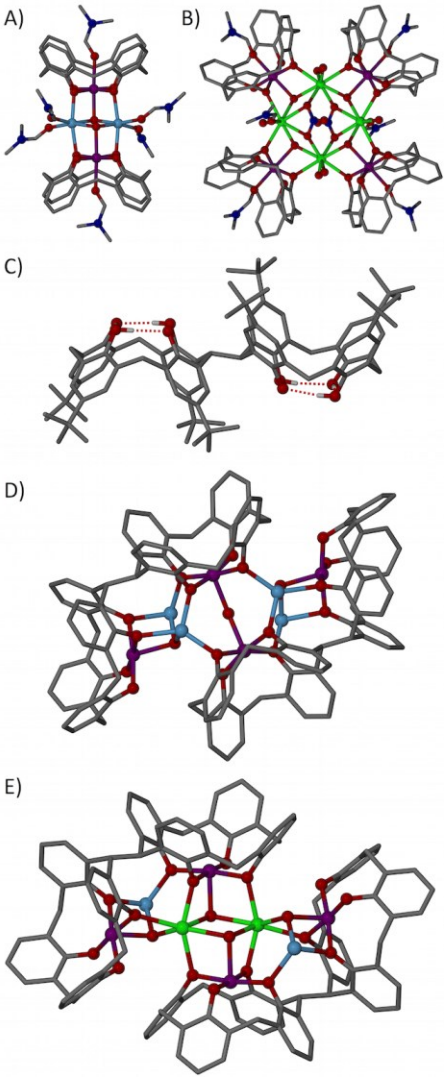

Figure 1. Single crystal *X*-ray structures of A) **1**, B) **2**, C) L1, D) **3**, and E) **4**.[3b, 5a, 11] Colour code C – grey, O – red, N – royal blue, Mn^{II} – pale blue, Mn^{III} – purple, Ln^{III} – green. Hydrogen atoms (except those involved in lower-rim H-bonding in C), ^{t}Bu groups of C[4] and L1 (except those shown in C), ligated solvent molecules in D and E, and co-crystallised solvent / anions omitted for clarity. Not to scale.

Here we show that variation in reactant stoichiometry has a remarkable effect on cluster synthesis with L1, the result being the formation of two new Mn_xLn_y (x = 10 / y=0, x=8 / y=2) clusters that are very closely related in structure to those shown in Figures 1D and 1E; the polymetallic cores of these new assemblies can essentially be thought of as 'expanded' versions of **3** and **4**, with addition of two Mn^{III} ions in both cases. These were obtained by increasing the ratios of the reacting species, and in one case also by altering crystallisation conditions.

Reaction of L1 with manganese(II) chloride in a DMF/MeOH mixture (in the presence of Et_3N as a base) afforded single crystals found to be of formula $[Mn^{III}_6Mn^{II}_4(L1\text{-}8H)_2(\mu_3\text{–}O)_2(\mu_3\text{–}OH)_2(\mu\text{–}CH_3O)_4(H_2O)_4(dmf)_8](dmf)_4]$ (**5,** Fig. 2) upon slow evaporation of the mother liquor. The crystals were found to be in a triclinic cell and structure solution was carried out in space group *P*-1.§ The asymmetric unit (ASU) comprises half of the cluster due to the presence of the inversion centre (located within the Mn5–O14–Mn5'-O14' rhomboid, Fig. 2A), thus only half of the assembly is described in detail.

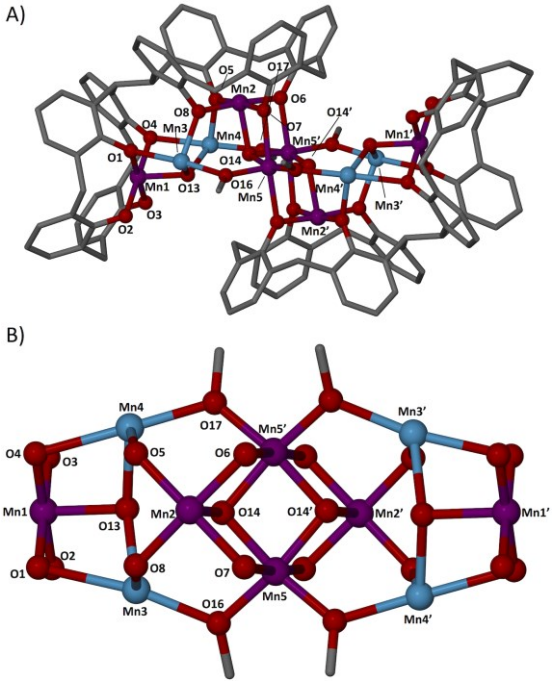

Figure 2. A) Single crystal *X*-ray structure of **5** with selected atoms labelled according to discussion. B) Top-down view of A showing the cluster core and the presence of a central Mn^{III}_4 butterfly. Colour code C – grey, O – red, N – royal blue, Mn^{II} – pale blue, Mn^{III} – purple. H atoms, ^{t}Bu groups of L1, ligated solvent molecules and co-crystallised solvent / anions are omitted for clarity. Figures not to scale.

Inspection of the structure shows that Mn1 is bound in a C[4] lower-rim tetraphenolic pocket (oxygen atoms O1–O4, Mn–O distances in the range of 1.907(5)-1.935(4) Å) and is in the 3+ oxidation state as expected based on C[4] binding rules. The coordination sphere of Mn1 is completed by a ligated dmf molecule (Mn1–O9, 2.35(3) Å) that resides within a C[4] cavity, as well as a μ_3-hydroxide (Mn1–O13, 2.107(5) Å) which bridges to Mn3 and Mn4 (Mn3–O13, 2.192(5) Å and Mn4–O13, 2.187(5) Å, Fig. 2B); the Jahn-Teller axis of Mn1 is defined by the O9-Mn1-O13 vector. Both Mn3 and Mn4 are in a 2+ oxidation state and, as is the case for **3** (Fig. 1D), they reside in the pockets between the constituent C[4] lower-rims of the L1 octa-anion. Mn3 is bonded to a dmf molecule (Mn3–O11, 2.163 Å), two μ–phenoxide oxygens (Mn3–O1, 2.436(4) Å and Mn3–O8, 2.109(4) Å), an aqua ligand (Mn3–O15, 2.241(5) Å) and a μ–methoxide (Mn3–O16, 2.154(5) Å). The coordination

spheres of Mn4 (2+) and Mn1 (3+) are near identical to those of Mn3 (2+) and Mn2 (3+) respectively, with only negligible differences observed in the bond lengths in both cases (Supporting Information). Mn5 is in a 3+ oxidation state and has distorted octahedral geometry with its Jahn-Teller axis lying along the O7-Mn5-O6' vector (Mn5–O7, 2.295 Å and Mn5–O6', 2.331 Å). Two μ_3-oxides and two μ-methoxides complete the Mn5 / Mn5' coordination spheres with Mn5–O14, Mn5-O14', Mn5–O16 and Mn5–O17 distances being 1.920(5), 1.921(5), 1.926(6) and 1.925(6) Å respectively. Structural comparison of **5** (Fig. 2) with **3** (Fig. 1D) shows that the $Mn^{III}_6Mn^{II}_4$ core in the former can best be described as an 'expanded' version of the previously reported $Mn^{III}_4Mn^{II}_4$ species.[11] As such, 'expansion' occurs with the incorporation of two additional methoxy–bridged Mn^{III} ions, forming the well-known butterfly-like motif in the centre of the cluster core.

Reaction of L1 with manganese(II) nitrate and gadolinium(III) nitrate in a DMF/MeOH mixture in the presence of Et_3N as a base, afforded single crystals of formula $[Mn^{III}_6Mn^{II}_2Gd^{III}_2(L_1–8H)_2(\mu_4–O)_2(\mu_3–OH)_2(\mu–OCH_3)_2(\mu–OH)_2(MeOH)_4(dmf)_8](NO_3)_2(H_2O)_2$ (**6**, Fig. 3) upon slow evaporation of the mother liquor. The crystals were found to be in a monoclinic cell and structure solution was carried out in the space group $P2_1/n$. The ASU comprises half of the cluster in which there is disorder relating to the position of the Mn^{II} and Gd^{III} ions; this has been modelled at half-occupancy and only one position is discussed below. Comparison of Figures 2 and 3 reveals that **6** is closely related to **5**, the only major difference being the interchange of one Mn^{II} for a Gd^{III} ion.

Mn1 is bound in a C[4] lower-rim tetraphenolic pocket (oxygen atoms O1–O4, Mn–O distances in the range of 1.920(5)-1.969(5) Å), is in a 3+ oxidation state and has distorted octahedral geometry (Fig. 3A). The coordination sphere is completed by a ligated dmf (Mn1–O9, 2.229(5) Å) in the C[4] cavity and a μ_3–OH^- (Mn1–O13, 2.174(6) Å, Fig. 3B); the O9-Mn1-O13 vector defines the Jahn-Teller axis with considerable variation from linearity (164.8(1)°), a feature likely attributable to the aforementioned disorder. The Mn3 ion is in the 2+ oxidation state and is disordered at half-occupancy across the two binding sites present between the constituent C[4] lower-rims. Mn3 has distorted octahedral geometry and, in addition to being coordinated to two phenolic oxygens (Mn3–O1, 2.346(4) Å and Mn3–O8, 2.193(4) Å), the coordination sphere is completed by a ligated dmf (Mn3–O11, 1.998(6) Å), a ligated MeOH (Mn3–O15, 2.246(5) Å), the aforementioned μ_3–OH^- (Mn3–O13, 2.184(7) Å) and a μ-hydroxide (Mn3–O17, 2.170(4) Å, bridging to Mn4). Gd1 is in the 3+ oxidation state, is heptacoordinate and has distorted pentagonal bipyramidal geometry. The coordination sphere comprises two phenoxides (Gd1–O4, 2.493(4) Å and Gd1–O5, 2.201(4) Å), a μ_3–hydroxide (Gd1–O13, 2.299(7) Å), a ligated dmf (Gd1–O12, 2.473(7) Å), a ligated methanol (Gd1–O16, 2.361(6) Å), a μ-methoxide (Gd1–O18, 2.184(5) Å, bridging to Mn4) and a μ_4–oxide (Gd1–O14, 2.497(4) Å, bridging to Mn4, Mn4' and Mn2). With the exception of coordination to O14, Mn2 (3+) has a near identical coordination sphere to Mn1 (3+), with only negligible differences observed in the bond lengths (Supporting Information). Finally, Mn4 is in a 3+ oxidation state and has distorted octahedral geometry with a Jahn-Teller axis lying along the O7-Mn4-O6' vector (Mn4–O7, 2.354(4) Å and Mn4–O6', 2.256(4) Å). The aforementioned μ_4-oxides and μ-methoxides complete the Mn4 / Mn4' coordination spheres with respective Mn4–O14, Mn4-O14', Mn4–O17 and Mn4–O18' distances of 1.925(4), 1.901(5), 1.914(5) and 1.917(4) Å.

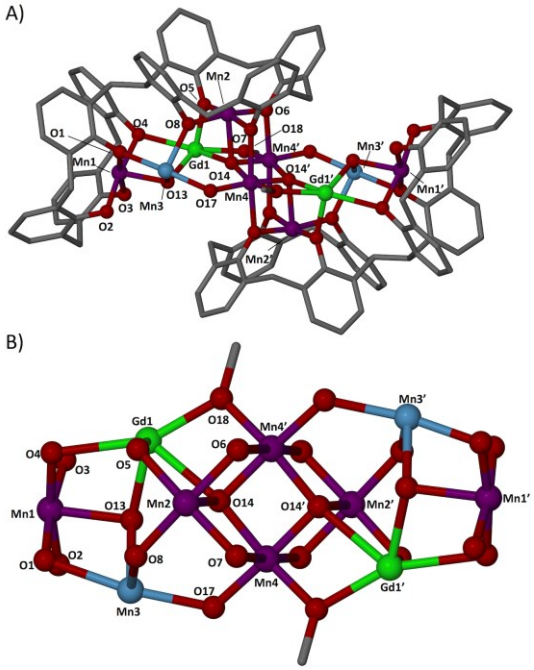

Figure 3. A) Single crystal *X*-ray structure of **6** with selected atoms labelled according to discussion. B) Top-down view of A showing the cluster core and the presence of a central Mn^{III}_4 butterfly. Only one position is shown for the disorder concerning Mn3 and Gd1 (Mn3A, Gd1A and associated disordered ligands hidden from view). Colour code C – grey, O – red, N – royal blue, Mn^{II} – pale blue, Mn^{III} – purple, Ln^{III} – green. H atoms, ^{t}Bu groups of L1, ligated solvent molecules and co-crystallised solvent / anions are omitted for clarity. Figures not to scale.

Comparison of Figure 2B and 3B shows that the cluster cores in **5** and **6** are near isostructural, the only major difference being the effective interchange of Mn^{II} for Gd^{III} ions (or Ln^{III} ions in general) in one binding site between the constituent C[4] lower-rims in each L1. This is remarkable considering the large overall changes required to move from **3** and **4** to **5** and **6** respectively, but is further evidence that analogous metal ion binding rules for bis-C[4] will closely mirror those of C[4]. In addition to this, the expected capping behaviour is also observed as shown in the cluster comparison in Figure S1. Examination of the extended structures of **5** and **6** reveals that the closest M…M distances are ~8.5 and ~14.2 Å respectively. The clusters in **6** are well isolated (Fig. S2), but the structure of **5** is interesting in that the assemblies pack closely so as to form chains along the *a* axis; this occurs as chains of intermolecular interactions. Inspection reveals a unique CH…O interaction between neighbouring aqua and dmf ligands, with a CH…O distance of 3.08 Å, as well as a unique CH…π interaction with a CH…aromatic centroid distance of 3.67 Å (Fig. S3, H atoms in staggered positions due to torsion shifts).

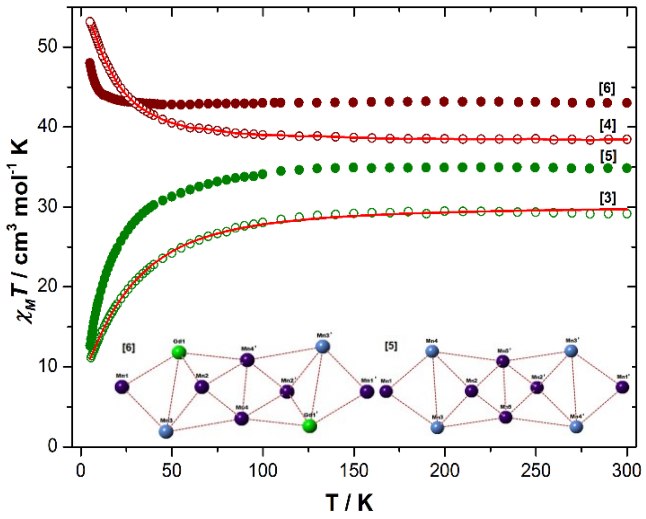

Figure 4. Experimental $\chi_M T$ *versus* T data for **3** - **6** measured in the T = 5 – 300 K temperature range in an applied field of 0.1 T.

The dc molar magnetic susceptibility, χ_M, of polycrystalline samples of **5** and **6** were measured in an applied magnetic field, B, of 0.1 T, over the 5 - 300 K temperature, T, range (Fig. 4, where $\chi = M / B$, and M is the magnetization). At room temperature, the $\chi_M T$ products of **5** and **6** have values of 34.9 and 43.02 cm^3 mol^{-1} K, respectively. These are in excellent agreement with those expected from the spin-only contributions to the magnetism of a [$Mn^{III}_6Mn^{II}_4$] (35.5 cm^3 mol^{-1} K) and [$Mn^{III}_6Mn^{II}_2Gd^{III}_2$] (42.5 cm^3 mol^{-1} K) moieties, with g = 2.00. On lowering the temperature the $\chi_M T$ value of **5** remains essentially unchanged to T = 100 K, where it begins to decrease more rapidly to a minimum value of 12.7 cm^3 mol^{-1} K at 5 K. Upon cooling, the $\chi_M T$ value of **6** remains practically constant to 50 K, from where there is a small increase until ~20 K, below which there is a more abrupt increase to a value of 48 cm^3 mol^{-1} K at 5 K. Due to the size and structural complexity of **5** and **6**, a quantitative fit of the susceptibility data is not possible. Qualitatively, the magnetic behaviour of **5** and **6** is similar to that of **3** [$Mn^{III}_4Mn^{II}_4$] and **4** [$Mn^{III}_4Mn^{II}_2Gd^{III}_2$], respectively, as can been seen from inspection of Figure 4. In the latter species three independent isotropic exchange parameters were obtained for both **3** ($J_{Mn(II)\text{-}Mn(III)}$ = +0.92 cm^{-1}; $J_{Mn(II)\text{-}Mn(II)}$ = -4.48 cm^{-1} and $J_{Mn(III)\text{-}Mn(III)}$ = -1.52 cm^{-1}) and **4** ($J_{Mn(III)\text{-}Gd(III)}$ = -0.062 cm^{-1}; $J_{Mn(II)\text{-}Gd(III)}$ = +0.066 cm^{-1} and $J_{Gd(III)\text{-}Gd(III)}$ = -0.061 cm^{-1}), revealing the existence of both ferro- and antiferromagnetic exchange interactions. Given the structural similarity of **5** and **6** to these previously published complexes it would seem safe to assume that a similar pattern of exchange exists. Variable-temperature-and-variable-field (VTVB) magnetization data is consistent with this picture in which M rises slowly with increasing B, failing to reach saturation in both cases (Fig. S4).

To conclude, we have shown that changes in reaction stoichiometry cause remarkable cluster core expansion in bis-calix[4]arene-supported cages. Both of the expansions shown here involve the analogous incorporation of two additional Mn^{III} ions, generating larger assemblies based on a generic butterfly-like {$Mn^{III}_2Mn^{III}_2(OH)_2$} core. This metallic addition, does not have a major impact in the magnetism, with the magnetic behaviour of **5** and **6,** akin to the previously reported **3** and **4**. The results presented suggest that other bis-C[4]-supported clusters may exhibit similar expansion behaviour, thereby allowing one to tune the resulting magnetic properties through extension of the metal ion binding rules established for C[4]. This will be studied and reported in due course.

Notes and references

‡ Compound L1 was synthesised according to literature procedure.[9] Single crystal *X*-ray data for **5** and **6** were collected on a Bruker D8 diffractometer operating a PHOTON 100 detector (shutterless scans) at 100(2) K and with synchrotron radiation (λ = 0.7749 Å). § **Crystal data for 5 (CCDC 1484325)**: $C_{216}H_{310}Mn_{10}N_{12}O_{40}$, dark violet plate, 0.1 x 0.06 x 0.01 mm^3, triclinic, space group *P*-1 (No. 2), a = 14.9101(5), b = 17.9438(5), c = 22.3792(7) Å, α = 69.512(2), β = 75.796(2), γ = 81.501(2)°, V = 5424.6(6) Å^3, Z = 1, $2\vartheta_{max}$ = 48.252°, 54412 reflections collected, 13284 unique (R_{int} = 0.0696). Final *GooF* = 1.045, *R1* = 0.1116, *wR2* = 0.2297. **Crystal data for 6 (CCDC 1484326):** $C_{206}H_{280}Mn_8Gd_2N_{10}O_{44}$, M = 4354.40, dark violet block, 0.4 x 0.35 x 0.3 mm^3, monoclinic, space group $P2_1/n$ (No. 14), a = 22.090(7), b = 19.1570(6), c = 27.0764(9) Å, β = 105.149(2)°, V = 11063.0(7) Å^3, Z = 2, $2\vartheta_{max}$ = 59.772°, 136715 reflections collected, 24604 unique (R_{int} = 0.0542). Final *GooF* = 1.077, *R1* = 0.1061, *wR2* = 0.2740.

1 a) M. Murrie, *Chem. Soc. Rev.*, 2010, **39**, 1986; b) R. Bagai, G. Christou, *Chem. Soc. Rev.*, 2009, **38**, 1011; c) L. N. Dawe, K. V. Shuvaev, L. K. Thompson, *Chem. Soc. Rev.*, 2009, **38**, 2334; d) R. E. P. Winpenny, *Chem. Soc. Rev.*, 1998, **27**, 447.

2 a) G. Aromí, E. K. Brechin, *Struct. Bonding*, 2006, **122**, 1; b) J.-N. Rebilly, T. Mallah, *Struct. Bonding*, 2006, **122**, 103.

3 a) C. Aronica, G. Chastanet, E. Zueva, S. A. Borshch, J. M. Clemente-Juan, D. Luneau, *J. Am. Chem. Soc.*, 2008, **130**, 2365; b) G. Karotsis, S. J. Teat, W. Wernsdorfer, S. Piligkos, S. J. Dalgarno, E. K. Brechin, *Angew. Chem. Int. Ed.*, 2009, **48**, 8285; c) S. M. Taylor, G. Karotsis, R. D. McIntosh, S. Kennedy, S. J. Teat, C. M. Beavers, W. Wernsdorfer, S. Piligkos, S. J. Dalgarno, E. K. Brechin, *Chem. Eur. J.*, 2011, **17**, 7521; d) G. Karotsis, S. Kennedy, S. J. Dalgarno, E. K. Brechin, *Chem. Commun.* 2010, **46**, 3884.

4 S. Sanz, R. D. McIntosh, C. M. Beavers, S. J. Teat, M. Evangelisti, E. K. Brechin, S. J. Dalgarno, *Chem. Commun.*, 2012, **48**, 1449.

5 a) G. Karotsis, S. Kennedy, S. J. Teat, C. M. Beavers, D. A. Fowler, J. J. Morales, M. Evangelisti, S. J. Dalgarno, E. K. Brechin, *J. Am. Chem. Soc.*, 2010, **132**, 12983; b) S. Sanz, K. Ferreira, R. D. McIntosh, S. J. Dalgarno, E. K. Brechin, *Chem. Commun.*, 2011, **47**, 9042.

6 M. Coletta, E. K. Brechin, S. J. Dalgarno, in *Calixarenes and Beyond*, ed. P. Neri, J. L. Sessler and M. –X. Wang, Springer International Publishing, Switzerland, 1st edn, 2016, ch. 25, pp 671–689.

7 E. K. Brechin, J. Yoo, M. Nakano, J. C. Huffman, D. N. Hendrickson, G. Christou, *Chem. Commun.*, 1999, 783.

8 M. A. Palacios, R. McLellan, C. M. Beavers, S. J. Teat, H. Weihe, S. Piligkos, S. J. Dalgarno, E. K. Brechin, *Chem. Eur. J.*, 2015, **21**, 11212.

9 L. T. Carroll, P. Aru Hill, C. Q. Ngo, K. P. Klatt, J. L. Fantini, *Tetrahedron*, 2013, **69**, 5002.

10 P. Murphy, S. J. Dalgarno, M. J. Paterson, *J. Phys. Chem. A*, 2014, **118**, 7986.

11 R. McLellan, M. A. Palacios, C. M. Beavers, S. J. Teat, S. Piligkos, E. K. Brechin, S. J. Dalgarno, *Chem. Eur. J.*, 2015, **21**, 2804.

